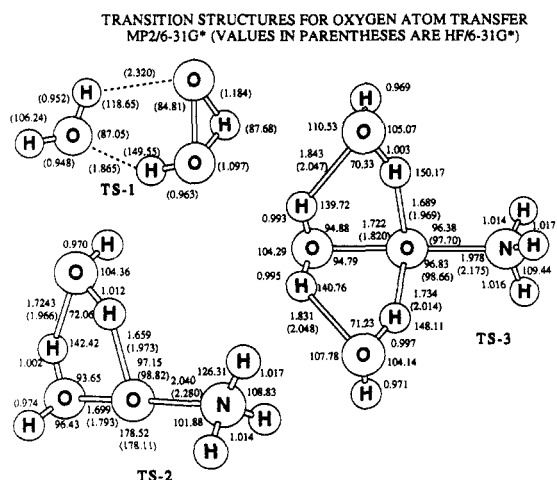


Table I. Barriers^a Relative to Isolated Reactants for NH₃ + H₂O₂ + n(H₂O) [n = 0, 1, 2]

	HF/6-31G*// HF/6-31G*	MP4/6-31G*// HF/6-31G* ^b	MP2/6-31G*// MP2/6-31G* ^c	MP4/6-31G*// MP2/6-31G* ^{b,c}
(n = 0) ^d	41.7	52.1 ^e	57.5	51.4 ^f
TS-2 (n = 1)	28.8	31.8	34.6	29.4 (39.1) ^g
TS-3 (n = 2)	18.5	14.9	16.0	11.2 (33.1) ^h

^a In kilocalories per mole. ^b All MP4 calculations used a frozen core and include single, double, triple, and quadruple excitations. ^c All MP2 calculations used full orbital space. ^d See ref 8 for transition structure. ^e The barrier relative to the H₂O₂-NH₃ linear complex is 62.9 kcal/mol.⁸ ^f The barrier relative to the water oxide + NH₃ cyclic complex is 24.3 kcal/mol.⁸ ^g The barrier relative to the H₂O₂-H₂O complex and isolated NH₃. ^h The barrier relative to the H₂O₂-2H₂O complex and isolated NH₃.

proximal oxygen (α -oxygen of the ROOH) effecting a formal 1,4-hydrogen shift as depicted in TS-2. The reaction path for



oxygen transfer to NH₃ was followed in internal coordinates¹² and led from TS-2 back to solvated water oxide and ammonia, supporting a simple protonation-deprotonation pathway. Although a remarkable decrease in the ΔE^\ddagger results from this water catalysis (TS-2),¹³ the barrier of 29.4 kcal/mol relative to the isolated reactants and 39.1 from hydrogen-bonded H₂O₂ would still be much too high to be commensurate with the oxygen donation potential of native 1a. We therefore employed a second water molecule (TS-3), and the barrier for oxygen atom transfer from hydrogen peroxide and two isolated water molecules dropped to 11.2 kcal/mol for an overall decrease in activation energy of 40.2 kcal/mol.¹³ A decrease in barrier of 18.3 kcal/mol for H₂O₂ relative to H₂O₂ + 2H₂O reflects the energy difference of 28.9 kcal/mol for the H₂O₂-2H₂O complex and water oxide solvated by two water molecules. More significantly, the barrier for oxygen transfer (TS-3) from solvated water oxide is only 4.2 kcal/mol, which falls in an energy range that would be consistent with the extremely high oxidizing capacity exhibited by native 1a. Such a dramatic energy decrease is far in excess of that which would be anticipated on the basis of simple hydrogen bonding.¹⁴

Although the reduction in the barrier must reflect both the amelioration of the 1,2-hydrogen shift barrier and a decrease in electron density at the "electrophilic" oxygen, the greatest effect comes from stabilization of water oxide itself by the water molecules.¹³ Since alkyl hydrogen peroxide 1b has been established to be 10⁴ times more reactive than H₂O₂ as an oxygen donor,⁷ comparable inductive effects should further lower the energy of TS-3. The present study strongly suggests that a simple S_N2 displacement (eq 1) cannot account for the oxygen donation potential of 1a. *The oxygen transfer process requires an oxenoid*

oxygen atom and a neutral leaving group. The hydrogen transfer can also be achieved by simple protonation-deprotonation circumventing the more energetically demanding 1,2-hydrogen shift. We therefore suggest that hydrogen bonding by the N₃ hydrogen on one side¹⁵ and one (or two) water molecule(s) on the other would afford a transition structure in native flavin 1a that resembles TS-3, providing a novel explanation for the unusual monooxygenase reactivity of flavins. Hence, the potentially ex-orbitant barrier for this overall process may be abated by the stabilizing influence of one or more water molecules.¹⁶ The data in the present study also strongly suggests that a structure resembling TS-3 is involved in a great many reactions of hydrogen peroxide in protic solvents.

Acknowledgment. This work was supported in part by a grant from the National Science Foundation (CHE-87-11901), the National Institutes of Health (CA 47348-02), and Ford Motor Company. We are also thankful to the Pittsburgh Supercomputing Center, Ford Motor Company, and the Computing Center at Wayne State University for generous amounts of computing time.

Registry No. NH₃, 7664-41-7; H₂O₂, 7722-84-1; H₂O, 7732-18-5.

(15) The importance of five-membered intramolecular hydrogen bonding in α -azo hydroperoxides has been firmly established to play a major role in oxygen atom transfer: Baumstark, A. L.; Vasquez, P. C. *J. Org. Chem.* **1987**, *52*, 1939.

(16) For a discussion of solvent-assisted proton transfer in alkyl hydrogen peroxides, see: (a) Dankleff, M. A. P.; Ruggero, C.; Edwards, J. O.; Pyun, H. Y. *J. Am. Chem. Soc.* **1968**, *90*, 3209. (b) Swern, D. *Organic Peroxides*; Wiley Interscience: New York, 1971; Vol. II, pp 73-74.

Theoretical Study of Oxygen Atom Transfer. The Role of Electron Correlation

Robert D. Bach,* Joseph J. W. McDouall, Amy L. Owensby, and H. Bernhard Schlegel

*Department of Chemistry, Wayne State University
Detroit, Michigan 48202*

Received November 13, 1989

The transfer of an oxygen atom involving cleavage of an oxygen-oxygen σ bond is one of the most significant biological transformations known,¹ and this type of oxidative insertion also enjoys a unique status in synthetic organic chemistry.² Despite the generality of such reactions, the literature is essentially void of high level ab initio calculations involving oxygen transfer where an O-O bond is involved.³ Pople et al. reported⁴ that a 1,2-

(1) (a) Walsh, C. In *Flavins and Flavoproteins*; Vincent, M., Williams, C. H., Eds.; Elsevier/North Holland: Amsterdam, 1981; pp 121-132. (b) Walsh, C. In *Enzymatic Reaction Mechanisms*; W. H. Freeman and Co.: San Francisco, 1979; pp 406-463. (c) Bruce, T. C. In *Flavins and Flavoproteins*; Bray, R. C., Engel, P. C., Mayhew, S. E., Eds.; Walter DeGruyter and Co.: New York, 1984; pp 45-55.

(2) (a) Finn, M. G.; Sharpless, K. B. *Asymmetric Synth.* **1985**, *5*, 247. (b) Sheldon, R. A.; Kochi, J. *Metal-Catalyzed Oxidations of Organic Compounds*; Academic Press: New York, 1981; Chapter 9. (c) Mimoun, H.; Chaumette, P.; Mignard, M.; Saussine, L. *Nouv. J. Chim.* **1983**, *7*, 467.

(3) For a highly detailed theoretical study of the reaction of ozone with alkenes, see: Cremer, D.; Bock, C. W. *J. Am. Chem. Soc.* **1986**, *108*, 3375 and references therein.

(12) Gonzalez, G.; Schlegel, H. B. *J. Chem. Phys.* **1989**, *90*, 2154.

(13) Water oxide complexed by one water molecule in a cyclic array resembling that in TS-2 exists at an energy minimum that is stabilized by 21.6 kcal/mol. The hydrogen-bonded bicyclic array, involving two water molecules, is 42.7 kcal/mol lower in energy than its separated entities and only 7.0 kcal/mol above the energy of isolated H₂O₂ plus two water molecules.

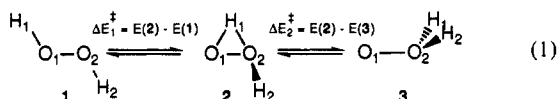
(14) For example, the enthalpy values for the formation of water dimer at the MP4SDTQ/6-31G*//HF/6-31G* and MP4/6-31+G(2d,2p) levels are -7.4 and -3.6 kcal/mol, respectively: Del Bene, J. E. *J. Phys. Chem.* **1988**, *92*, 2874. At the former level the hydrogen-bonding stabilization of H₂O₂ and H₂O is 9.3 kcal/mol.

Table I. Optimized Geometry of the Transition State and Energies for the 1,2-Hydrogen Shift of Hydrogen Peroxide

	HF/6-31G*	MP2/6-31G*	MP4SDTQ/6-31G*	HF/6-31G**	HF/6-311++G(2d,2p)
$r(\text{O}_1\text{O}_2)^a$	1.602	1.576	1.633	1.601	1.588
$r(\text{O}_1\text{H}_1)$	1.190	1.426	1.425	1.184	1.187
$r(\text{O}_2\text{H}_1)$	1.094	1.035	1.038	1.081	1.083
$r(\text{O}_2\text{H}_2)$	0.951	0.980	0.980	0.947	0.943
$\angle\text{O}_1\text{O}_2\text{H}_2$	100.49	98.57	96.89	101.01	101.53
$\angle\text{H}_1\text{O}_1\text{O}_2\text{H}_2$	106.04	104.06	104.22	106.77	105.33
ΔE_1^{\ddagger} ^b	57.5	58.0		55.1	56.8
ΔE_2^{\ddagger}	18.0	4.7		15.6	17.6
ΔE_1^{\ddagger} MP4	45.8	54.0	53.4	43.6	45.1
ΔE_2^{\ddagger} MP4	-1.3	3.9	3.7	-4.0	0.1

^a Bond lengths in angstroms; angles in degrees. ^b Relative energies in kilocalories per mole (including ΔZPE) with geometry optimized at the level indicated; MP2 energies are full; MP4 energies are frozen core.

hydrogen shift in H_2O_2 to form water oxide (eq 1) has a surprisingly high barrier ($\Delta E_1^{\ddagger} = 59.2$) with a transition structure that is 18.8 kcal/mol above the energy of water oxide with the HF/6-31G** level. However, at the MP4SDQ/6-31G**//



HF/6-31G* level, with the E_{4T} triples contribution to the correlation energy calculated with the 6-31G* basis, the barrier for reversion of water oxide to H_2O_2 (ΔE_2^{\ddagger}) is eliminated entirely. It was concluded that water oxide cannot exist. When the triples contribution to the MP4 energy barrier is calculated with the same basis set, a small negative barrier ($\Delta E_2^{\ddagger} = -0.9$ kcal/mol) is still obtained for the reverse reaction.⁵ As noted in Table I, the potential-energy surface for the 1,2-hydrogen shift remains almost unchanged at the Hartree-Fock level over a broad range of basis sets up to and including the 6-311++G(2d,2p) basis. With this highly polarized basis set, the water oxide barrier (ΔE_2^{\ddagger}) is 20.8 kcal/mol. However, with fourth-order Møller-Plesset correlation corrections applied to the HF geometries, ΔE_2^{\ddagger} is significantly reduced and zero point energy corrections place the energy of water oxide nearly equal to or above the energy of the transition structure for all three cases where the geometry was optimized at the Hartree-Fock level.

Because of the computational expense involved, typical protocol is to calculate the correlation correction using a Hartree-Fock optimized geometry. The marked effect of correlation correction on the relative energy of water oxide suggested that Hartree-Fock theory gave a poor representation of both the O-O single bonds and the zwitterionic structure. When the structures were reoptimized at the MP2/6-31G* level, we found a radically different energy profile (Table I). The MP4SDTQ/6-31G**//MP2/6-31G* barrier for the hydrogen shift is 56.0 kcal/mol. Significantly, water oxide exists as a local minimum 6.3 kcal/mol below the energy of the transition structure, although with ΔZPE this barrier is reduced to 3.1 kcal/mol. Thus, water oxide does exist and could potentially serve as a donor of singlet oxygen atoms. At the MP2 level the O-O bond distance in H_2O_2 is now in agreement with experiment (1.469 vs 1.475 Å)⁴ and the O-O bond in water oxide is considerably shortened (0.09 Å) while the O-H bond in **2** is lengthened (0.24 Å). Optimization at the MP4/6-31G* level did not result in a meaningful improvement over the MP2 potential-energy surface, suggesting that the MP2 optimization is adequate.

The concerted transfer of an oxygen atom from H_2O_2 to NH_3 involves both a 1,2-hydrogen shift and the simultaneous transfer of the oxygen by an $\text{S}_{\text{N}}2$ -like cleavage of the O-O bond. The

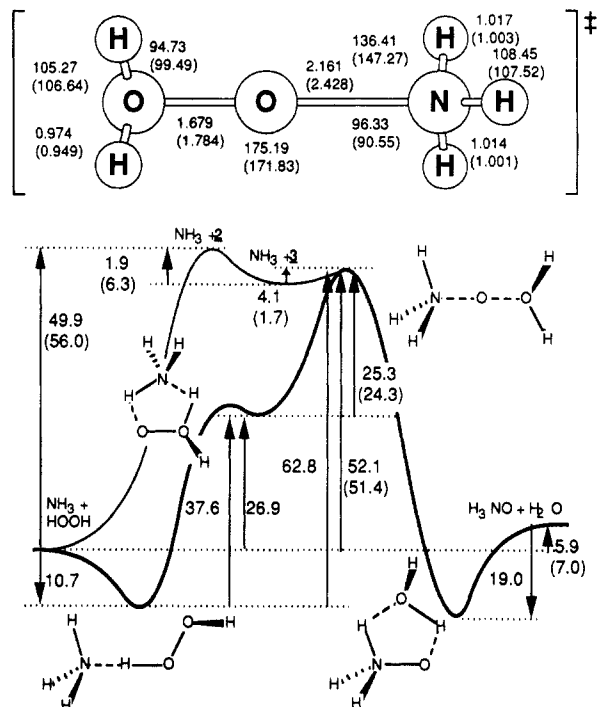


Figure 1. Top: Optimized transition-state structure for $\text{HOOH} + \text{NH}_3 \rightarrow \text{H}_2\text{O} + \text{H}_3\text{NO}$ at the MP2/6-31G* level (HF/6-31G* geometry in parentheses). Bottom: A comparison of the potential-energy profiles for 1,2-hydrogen shift in H_2O_2 and oxygen transfer from H_2O_2 to NH_3 at the MP4SDTQ/6-31G**//HF/6-31G* level in kilocalories per mole (no ΔZPE); MP4 energies using MP2 optimized geometries in parentheses.

transition structure (a first-order saddle point confirmed by a HF/6-31G* frequency calculation) has the hydrogen completely shifted and closely resembles water oxide and ammonia (Figure 1). In fact, the barrier calculated (MP4SDTQ/6-31G**//MP2/6-31G*) from ground-state water oxide plus ammonia is only 1.7 kcal/mol while the barrier for water oxide solvated by ammonia is 24.3 kcal/mol. The overall gas-phase barrier for oxygen transfer from H_2O_2 to NH_3 of 51.4 kcal/mol is lower than the 1,2-hydrogen shift barrier in H_2O_2 (56.0 kcal/mol, no ΔZPE) but only if the geometry is optimized at the MP2 level. When the reaction path is followed back from the transition state,⁶ it leads to water oxide plus ammonia, which strongly suggests that this is a two-step process. The most significant geometry changes are in the N-O and O-O bonds of the transition structure where the calculated MP2 bonds are shorter than the Hartree-Fock by as much as 0.27 Å. However, the magnitudes of these gas-phase barriers are simply too high to be compatible with oxygen-transfer chemistry in aqueous solution or in the presence of protic solvent. This suggests that oxygen atom transfer from either H_2O_2 or ROOH under typical experimental conditions must involve a protonation-deprotonation step affording an oxy-oxonium ion species resembling **3** prior to attack by the oxygen acceptor.

(4) Pople, J. A.; Raghavachari, K.; Frisch, M. J.; Binkley, J. S.; Schleyer, P. v. R. *J. Am. Chem. Soc.* **1983**, *105*, 6389.

(5) (a) Molecular orbital calculations have been carried out by using GAUSSIAN 88: Frisch, M. J.; Head-Gordon, M.; Schlegel, H. B.; Raghavachari, K.; Binkley, J. S.; Gonzales, C.; DeFrees, D. J.; Fox, D. J.; Whiteside, R. A.; Seeger, R.; Melius, C. F.; Baker, J.; Martin, R. L.; Kahn, R. L.; Stewart, J. J. P.; Fluder, E. M.; Topiol, S.; Pople, J. A. Gaussian, Inc., Pittsburgh, PA, 1988.

(6) Gonzalez, C.; Schlegel, H. B. *J. Chem. Phys.* **1989**, *90*, 2154.

In summary, we have established the importance of geometry optimization with electron correlation in the 1,2-hydrogen shift in H_2O_2 and in the gas-phase oxygen transfer from hydrogen peroxide to ammonia. The "electrophilic" oxygen atom has a full octet of electrons around oxygen in the transition state, and the leaving group is essentially neutral water.

Acknowledgment. This work was supported in part by a grant from the National Science Foundation (CHE-87-11901), the National Institutes of Health (CA 47348-02), and Ford Motor Company. We are also thankful to the Pittsburgh Supercomputing Center, the Ford Motor Company, and the Computing Center at Wayne State University for generous amounts of computing time.

Registry No. H_2O_2 , 7722-84-1; NH_3 , 7664-41-7.

X-ray Absorption Spectroscopic Structural Investigations of the Ni Site in Reduced *Thiocapsa roseopersicina* Hydrogenase

Michael J. Maroney,^{*,†,‡} Gerard J. Colpas,[†] and Csaba Bagyinka[†]

Department of Chemistry and Program in Molecular and Cellular Biology, University of Massachusetts Amherst, Massachusetts 01003

Received May 30, 1990

Hydrogenases (H_2 ases) are key enzymes in anaerobic metabolism that catalyze the reversible oxidation of H_2 .^{1,2} Hydrogenases may be divided into three classes based on the composition of their inorganic cofactors. These classes are the Fe-only, Fe-Ni, and Fe-Ni-Se enzymes.³ The latter two classes of enzymes contain unusual redox-active Ni centers. EPR has been extensively employed to monitor the redox chemistry of the Ni site and reveals that oxidized (as isolated) enzymes display characteristic signals that have been assigned to tetragonal, formally Ni(III) complexes (forms A and B).⁴ Upon reduction, these signals disappear, and the signal arising from a two-electron-reduction product (form C) appears.⁴ Electron spin echo envelope modulation studies (ESEEM) have been performed on H_2 ases from *Thiocapsa roseopersicina*,⁵ *Methanobacterium thermoautotrophicum*,⁶ and *Desulfovibrio gigas*⁷ and indicate the presence of one N atom near the Ni center in *T. roseopersicina* and *M. thermoautotrophicum* F_{420} -reducing H_2 ase and in the *D. gigas* enzyme, but not in the *M. thermoautotrophicum* viologen-reducing enzyme. X-ray absorption spectra obtained on H_2 ases from chemotrophs have been interpreted in terms of largely S-donor environments,⁸ involving

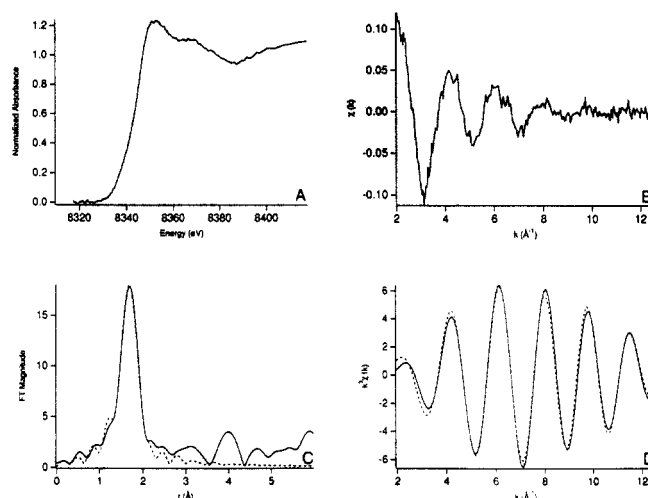


Figure 1. X-ray absorption spectra for the Ni center in *T. roseopersicina* hydrogenase (form C) (solid lines) and fits (dashed lines). Details of the fits are given in Table I. (A) The normalized Ni K-edge spectrum. (B) The unfiltered, base-line-corrected raw EXAFS spectrum. (C) Fourier transform of the EXAFS data over the k range 2-12.5 and the Fourier transform of the first coordination shell fit. (D) First coordination shell Fourier-filtered EXAFS and fit.

at least three and as many as six S-donor ligands. The lack of structure near the Ni K-edge in the *D. gigas* enzyme is consistent with either a 5- or 6-coordinate environment.⁹ These results contrast with recent EPR investigations employing ³³S-labeled H_2 ase from *Wolinella succinogenes* that are consistent with only one or two S-donor ligands in the first coordination sphere of Ni.¹⁰ We report here the analysis of XAS data obtained from the Fe-Ni H_2 ase from the purple photosynthetic bacterium, *T. roseopersicina*, poised in form C. These results provide the first information about the Ni-site structure of this key form of the enzyme and the first direct evidence for a mixed-ligand Ni environment in this class of H_2 ase.

T. roseopersicina was cultured and the H_2 ase isolated and assayed as previously described,¹¹ employing preparative electrophoresis in the final purification step. The enzyme was fully reduced by H_2 and then oxidized to form C by the addition of benzylviologen, using EPR spectroscopy to monitor the redox state of the Ni center. The sample used in the XAS studies was prepared in 20 mM Tris-HCl (pH 8) buffer containing 20% glycerol prior to concentration to ca. 0.3 mM Ni. The sample was analyzed for Fe and Ni content by graphite furnace atomic absorption spectroscopy following data collection and found to have an Fe:Ni ratio ((7 ± 1):1) consistent with published values.¹² X-ray fluorescence data was collected by using a 13-element Ge array detector from frozen solutions held at 77 K in a cryostat on beam line X9A at the National Synchrotron Light Source (2.53 GeV, ca. 110-180 mA) employing a monochromator with Si[111] crystals (resolution ca. 1 eV). Spectra were calibrated to the first inflection in a Ni foil spectrum. Transmission data from model compounds ($[Ni(Im)_6](BF_4)_2$ ¹³ and $(Et_4N)_2[Ni(p-SC_6H_4Cl)_4]$ ¹⁴) that were diluted with boron nitride to reduce thickness effects were collected at ambient temperature and employed in analyzing the protein data over the k range 2-12.5 using the amplitude and phase functions of McKale et al. that were calculated by using

(9) Eidsness, M. K.; Sullivan, R. J.; Scott, R. A. In *The Bioinorganic Chemistry of Nickel*; Lancaster, J. R., Ed.; VCH Publishers: New York, 1988; Chapter 4.

(10) Albracht, S. P. J.; Kröger, A.; van der Zwaan, J. W.; Uden, G.; Böcher, R.; Mell, H.; Fontijn, R. D. *Biochim. Biophys. Acta* 1986, 874, 116.

(11) (a) Kovacs, K. L.; Tigyi, G.; Alfonz, H. *Prep. Biochem.* 1985, 15, 321.

(b) Bagyinka, C.; Zorin, N. A.; Kovacs, K. L. *Anal. Biochem.* 1984, 142, 7.

(12) Bagyinka, C.; Szokefalvi-Nagy, Z.; Demeter, I.; Kovacs, K. L. *Biochem. Biophys. Res. Commun.* 1989, 162, 422.

(13) Van Ingen Schenau, A. D. *Acta Crystallogr.* 1975, B31, 2736.

(14) Rosenfield, S. G.; Armstrong, W. H.; Mascharak, P. M. *Inorg. Chem.* 1986, 25, 3014.

[†] Department of Chemistry.

[‡] Program in Molecular and Cellular Biology.

(1) Adams, M. W. W.; Mortenson, L. E.; Chen, J.-S. *Biochim. Biophys. Acta* 1981, 594, 105.

(2) Vignais, P. M.; Colbeau, A.; Willison, J. C.; Jouanneau, Y. *Adv. Microb. Physiol.* 1985, 26, 155.

(3) Fauque, G.; Peck, H. D., Jr.; Moura, J. J. G.; Huynh, B. H.; Berlier, Y.; DerVartanian, D. V.; Teixeira, M.; Przybyla, A. E.; Lespinat, P. A.; Moura, I.; LeGall, J. *FEMS Microbiol. Rev.* 1988, 54, 299.

(4) (a) Cammack, R.; Bagyinka, C.; Kovacs, K. L. *Eur. J. Biochem.* 1989, 182, 357. (b) Cammack, R.; Fernandez, V. M.; Schneider, K. In *The Bioinorganic Chemistry of Nickel*; Lancaster, J. R., Ed.; VCH Publishers: New York, 1988; Chapter 8. (c) Moura, J. J. G.; Teixeira, M.; Moura, I.; LeGall, J. *Ibid.* Chapter 9.

(5) Cammack, R.; Kovacs, K. L.; McCracken, J.; Peisach, J. *Eur. J. Biochem.* 1989, 182, 363.

(6) Tan, S. L.; Fox, J. A.; Kojima, N.; Walsh, C. T.; Orme-Johnson, W. H. *J. Am. Chem. Soc.* 1984, 106, 3064.

(7) Chapman, A.; Cammack, R.; Hatchikian, C. E.; McCracken, J.; Peisach, J. *FEBS Lett.* 1988, 242, 134.

(8) (a) Scott, R. A.; Wallin, S. A.; Czechowski, M.; DerVartanian, D. V.; LeGall, J.; Peck, H. D., Jr.; Moura, I. *J. Am. Chem. Soc.* 1984, 106, 6864.

(b) Scott, R. A.; Czechowski, M.; DerVartanian, D. V.; LeGall, J.; Peck, H. D., Jr.; Moura, I. *Rev. Port. Quim.* 1985, 27, 67. (c) Lindahl, P. A.; Kojima, N.; Hausinger, R. P.; Fox, J. A.; Teo, B. K.; Walsh, C. T.; Orme-Johnson, W. H. *J. Am. Chem. Soc.* 1984, 106, 3062.